PERGAMON Computers and Mathematics with Applications 39 (2000) 123–137

An International Journal
computers & mathematics with applications

www.elsevier.nl/locate/camwa

Circumventing the Ill-Conditioning Problem with Multiquadric Radial Basis Functions: Applications to Elliptic Partial Differential Equations

E. J. KANSA
Embry-Riddle Aeronautical University
Oakland, CA 94621, U.S.A.

Y. C. HON
Department of Mathematics
City University of Hong Kong
Kowloon, Hong Kong

(Received June 1999; accepted July 1999)

Abstract—Madych and Nelson [1] proved multiquadric (MQ) mesh-independent radial basis functions (RBFs) enjoy exponential convergence. The primary disadvantage of the MQ scheme is that it is global, hence, the coefficient matrices obtained from this discretization scheme are full. Full matrices tend to become progressively more ill-conditioned as the rank increases.

In this paper, we explore several techniques, each of which improves the conditioning of the coefficient matrix and the solution accuracy. The methods that were investigated are

(1) replacement of global solvers by block partitioning, LU decomposition schemes,
(2) matrix preconditioners,
(3) variable MQ shape parameters based upon the local radius of curvature of the function being solved,
(4) a truncated MQ basis function having a finite, rather than a full band-width,
(5) multizone methods for large simulation problems, and
(6) knot adaptivity that minimizes the total number of knots required in a simulation problem.

The hybrid combination of these methods contribute to very accurate solutions.

Even though FEM gives rise to sparse coefficient matrices, these matrices in practice can become very ill-conditioned. We recommend using what has been learned from the FEM practitioners and combining their methods with what has been learned in RBF simulations to form a flexible, hybrid approach to solve complex multidimensional problems. © 2000 Elsevier Science Ltd. All rights reserved.

Keywords—Multiquadric radial basis functions applied to PDEs, Two-dimensional Poisson elliptic partial differential equations, Domain decomposition methods for systems of linear equations, Truncated multiquadric radial basis functions, Multizone decomposition methods.

The authors wish to acknowledge the helpful suggestions of C. S. Chen, University of Nevada at Las Vegas, regarding the construction of a compactly supported MQ basis function. The work described in this paper was partially supported by a grant from the the Research Grants Council of the Hong Kong Special Administrative Region, China (Project No. 9040428) and a grant from the City University of Hong Kong (Project No. 7000943).

0898-1221/00/$ - see front matter © 2000 Elsevier Science Ltd. All rights reserved. Typeset by AMS-TEX
PII: S0898-1221(00)00071-7

1. INTRODUCTION

The numerical solution of partial differential equations (PDEs) has been dominated by either finite difference methods (FDM), finite element methods (FEM), or finite volume methods (FVM). These methods require a mesh to support the localized approximations; the construction of a mesh in three or more dimensions is a nontrivial problem. Only the function is continuous across meshes, but not the partial derivatives except for more complicated FEM schemes. These methods are not splines and the discontinuity of the derivative approximations can adversely affect wave propagation, etc.

In practice, only low-order approximations are used because of the notorious polynomial snaking problem. While higher-order schemes are necessary for more accurate approximations of the spatial derivatives, they are not sufficient without monotonicity constraints. Because of the low-order schemes typically employed, the spatial truncation errors can only be controlled by using progressively smaller meshes. The mesh spacing, h, must be sufficiently fine to capture the function's partial derivative behavior and to avoid unnecessarily large amounts of unphysical numerical artifacts contaminating the solution.

Spectral methods typically require the construction of a tensor-product mesh using the zeros of a higher-order polynomial such as the Chebyshev polynomial. However, the primary disadvantages of such schemes are that the domain must be regular to obtain the tensor product mesh, and the knots are restricted to the loci of the zeros of these polynomials. Whether FDM, FEM, FVM, or spectral methods are used, they all suffer from the curse of dimensionality.

The physical world will have domains that are highly irregular and not strictly convex. It would be extremely desirable to be able to solve PDEs over an extremely irregular domain, and discretize the domain without any structure to the knots. The use of standard methods in complex simulations has not only the curse of dimensionality, but the need for very fine meshing in certain localities, and the need for complex programming algorithms. The low rate of convergence of standard methods requires ever increasingly bigger, faster, and expensive computers.

Franke [2] has reported the results of a comprehensive study of scattered data interpolation methods that were compared with analytic two-dimensional test functions. In summary, he found those scattered data schemes having local compact support were inferior in performance on several criteria. However, the global RBF schemes such as Hardy's [3,4] MQ and Duchon's [5] thin-plate spline schemes performed optimally. The debate whether compactly or globally supported basis functions has not been sufficiently resolved especially for large complex problems.

Kansa [6,7] introduced the concept of solving PDEs using RBFs for hyperbolic, parabolic, and elliptic PDEs with RBFs. Considering Franke's results, he focused upon the MQ-RBFs and argued that PDEs are intrinsically related to the interpolation scheme from which PDE solvers are derived. Kansa [6,7], Golberg and Chen [8], and Sharan *et al.* [9] show dramatic efficiencies with the exponentially convergent MQ scheme. For example, Golberg and Chen [10] showed that the solution of a three-dimensional Poisson equation can be solved with only 60 randomly distributed knots to the same degree of accuracy as a FEM solution with 71,000 linear elements.

Hon *et al.* [11–15] further extended the use of the MQ-RBFs on the numerical solutions of various ordinary and partial differential equations including general initial value problems [11], complicated biphasic mixture model for tissue engineering problems [12], nonlinear Burgers' equation with shock wave [13], shallow water equation for tide and currents simulation under irregular boundary [14], and free boundary problems like American option pricing [15]. The computations showed the definite advantages in using this truly mesh-free MQ-RBFs for solving various initial and boundary values problems.

The convergence proofs in applying the RBFs for scattered data interpolation was given by Wu [16] and recently on solving PDEs by Wu [17]. In the papers, two important features of the RBFs method had been observed:

(1) it is a truly mesh-free algorithm, and

(2) it is space dimension independent in the sense that the convergence order is of $O(h^{d+1})$ where h is the density of the collocation points and d is the spatial dimension.

In other words, as the spatial dimension of the problem increases, the convergence order also increases, and hence, much fewer scattered collocation points will be needed to maintain the same accuracy compared with FDM, FEM, and FVM. This shows the applicability of the RBFs for solving high-dimensional problems.

While Dubal *et al.* [18] noted many benefits of using MQ-RBFs to solve the initial conditions for a three-dimensional nonlinear Poisson equation, they solved the entire set of PDEs directly without the use of domain decomposition or block decomposition schemes. They noted the matrix resulting using nearly 2000 knots was extremely ill-conditioned.

In this paper, we do not recommend the direct solution of the global system of equations. Rather, we recommend a hybrid approach that permits a high degree of parallelization while simultaneously addressing the problems of ill-conditioning on several levels.

2. BACKGROUND

There exist an infinite class of RBFs. A radial basis function, $g(\mathbf{x})$, $\mathbf{x} \in R^n$, depends only upon the radial (usually Euclidean) distances between the knots, $(\mathbf{x}_j)$. RBFs can have either global or compact support.

The most commonly used global RBFs are

$$\text{Gaussians: } \exp\left(-\frac{(\mathbf{x}-\mathbf{x}_j)^2}{\sigma_j}\right), \tag{1}$$

$$\text{Thin-plate splines: } (\mathbf{x}-\mathbf{x}_j)^2 \log(\mathbf{x}-\mathbf{x}_j), \tag{2}$$

$$\text{Multiquadrics: } \left((\mathbf{x}-\mathbf{x}_j)^2 + c_j^2\right)^{1/2}. \tag{3}$$

Because of the exponential convergence properties of MQ, see [1], this study will concentrate upon MQ-RBFs. It is a simple matter to replace MQ-RBFs if an even better RBF is found.

Hardy's [4] interpolation scheme upon which the PDE collocation is based is as follows:

$$F(\mathbf{x}_i) = F_i = \sum_j \alpha_j g_{ij} + \sum_k \beta_k p_k(\mathbf{x}_i), \tag{4}$$

$$0 = \sum_j \alpha_j p_k(\mathbf{x}_i), \qquad (1 \le k \le M), \tag{5}$$

which can be expressed as

$$\mathbf{\Phi} = \begin{bmatrix} \mathbf{G} & \mathbf{P} \\ \mathbf{P}^\top & \mathbf{0} \end{bmatrix} \begin{bmatrix} \boldsymbol{\alpha} \\ \boldsymbol{\beta} \end{bmatrix} = \mathbf{H}\gamma, \tag{6}$$

where F is specified at N scattered data centers, $\mathbf{x}_i$, and there are M constraint equations, $\mathbf{G}$ is an $N \times N$ matrix consisting of elements $[g(\mathbf{x}_i - \mathbf{x}_j)] = g_{ij}$, where $g(\mathbf{x}-\mathbf{x}_j) = ((\mathbf{x}-\mathbf{x}_j)^2 + c_j^2)^{1/2}$, $\mathbf{P}$ is an $N \times M$ matrix consisting of polynomials, $p_k(\mathbf{x}_i)$, $\mathbf{0}$ is an $M \times M$ matrix consisting of zero elements, $\mathbf{\Phi} = [F_1, \ldots, F_N, 0, \ldots, 0]^\top$, and $\gamma = [\alpha_1, \ldots, \alpha_N, \beta_1, \ldots, \beta_M]^\top$. In practice, $M = 1$ and $p_1(\mathbf{x}_i) = 1$.

The unknown expansion coefficients, γ, are found by specifying $\mathbf{\Phi}$ at the knots, $(\mathbf{x}_j)$, and inverting the matrix, $\mathbf{H}$. That is,

$$\gamma = \mathbf{H}^{-1}\mathbf{\Phi}(\mathbf{x}_i). \tag{7}$$

The procedure for solving PDEs is based upon the interpolation expansion of $\mathbf{\Phi}$ using the fact that the spatial function is continuous differentiable. The spatial partial derivatives of $\mathbf{\Phi}$ can be

written compactly as

$$\mathbf{\Phi}_x(\mathbf{x}_i) = \mathbf{H}_x(\mathbf{x}_i)\gamma, \tag{8}$$

$$\mathbf{\Phi}_y(\mathbf{x}_i) = \mathbf{H}_y(\mathbf{x}_i)\gamma, \tag{9}$$

$$\mathbf{\Phi}_{xx}(\mathbf{x}_i) = \mathbf{H}_{xx}(\mathbf{x}_i)\gamma, \tag{10}$$

$$\mathbf{\Phi}_{xy}(\mathbf{x}_i) = \mathbf{H}_{xy}(\mathbf{x}_i)\gamma, \tag{11}$$

$$\mathbf{\Phi}_{yy}(\mathbf{x}_i) = \mathbf{H}_{yy}(\mathbf{x}_i)\gamma. \tag{12}$$

For example, the matrix elements of $\mathbf{H}_x$ are composed of elements

$$g_x(\mathbf{x}_i - \mathbf{x}_j) = \frac{(\mathbf{x}_i - \mathbf{x}_j)}{g(\mathbf{x}_i - \mathbf{x}_j)}; p_x(\mathbf{x}_i) \tag{13}$$

that are formed from the rules of calculus.

If $\mathbf{\Phi}$ varies in time, then it is assumed that there exists a local Gallelian frame in which the temporal and spatial variables are separable, or approximately separable. Then

$$\mathbf{\Phi}(\mathbf{x}, t) = \mathbf{H}(\mathbf{x})\gamma(t). \tag{14}$$

This paper will be restricted to two-dimensional elliptic Poisson PDEs. Assume that a domain is discretized at N knots, $(\mathbf{x}_j)$, that are in general, inhomogeneously scattered. However, RBFs also permit well structured data arrangements. On the boundary, $\partial\Omega$,

$$\mathbf{B}\mathbf{\Phi} = 0, \tag{15}$$

at M knots. In the interior, $\frac{\Omega}{\partial\Omega}$,

$$\mathbf{L}\mathbf{\Phi} = 0 \tag{16}$$

at $(N - M)$ knots. The operator, $\mathbf{B}$, can specify Dirichlet, Neumann, or Robin-type boundary conditions. The operator, $\mathbf{L}$, can represent a time dependent hyperbolic, parabolic, or elliptic PDE operator that is either linear or nonlinear in nature.

The elliptic problems studied here have the following form: let $\Omega = [0,1] \times [0,1]$,

$$\mathbf{L}\mathbf{\Phi} = \mathbf{\Phi}_{xx} + \mathbf{\Phi}_{yy} - k^2(\mathbf{\Phi})\mathbf{\Phi} = 0, \qquad \text{in } \frac{\Omega}{\partial\Omega}, \tag{17}$$

$$\mathbf{B}\mathbf{\Phi} = \mathbf{\Phi} - \mathbf{\Phi}(\partial\Omega) = 0, \qquad \text{on } \partial\Omega. \tag{18}$$

All that is required is a pointer system to distinguish interior knots from boundary knots. The test problems were constructed to have analytic solutions. Six possible analytic solutions that were studied are

$$F = \exp(ax + \mathrm{by}), \tag{19}$$

$$F = \cos(ax + \mathrm{by}), \tag{20}$$

$$F = \sin(ax + \mathrm{by}), \tag{21}$$

$$F = \log(ax + \mathrm{by} + 1.10^{-7}), \tag{22}$$

$$F = \exp\left(-a\left(x - \frac{1}{2}\right)^2 - b\left(y - \frac{1}{2}\right)^2\right), \tag{23}$$

$$F = \arctan(ax + \mathrm{by}). \tag{24}$$

In the test cases, either $a = b = 2$ or $a = b = 4$ were considered.

The procedure first requires the construction of a matrix

$$\mathbf{W} = \left[\mathbf{B}, \Delta^2\mathbf{H}\right]^\top, \tag{25}$$

and the forcing vector

$$\phi = \left[\mathbf{\Phi}, k^2\left(\mathbf{\Phi}\right)\mathbf{\Phi}\right]^\top. \tag{26}$$

The collocation problem is then a solution of the following set of linear equations:

$$\mathbf{W}\gamma = \phi. \tag{27}$$

The expansion coefficients, γ, are solved as

$$\gamma = \mathbf{W}^{-1}\phi. \tag{28}$$

Given the expansion coefficients, γ, $\mathbf{\Phi}_{\mathrm{MQ}}$ can be reconstructed everywhere over the domain as

$$\mathbf{\Phi}_{\mathrm{MQ}} = \mathbf{H}\gamma, \tag{29}$$

and the root-mean squared error shall be defined as

$$\mathrm{RMS} = \frac{1}{N}\sqrt{\Sigma\left(\frac{F_{\mathrm{MQ}}\left(\mathbf{x}_i\right) - F_{\mathrm{exact}}\left(\mathbf{x}_i\right)}{F_{\mathrm{exact}}\left(\mathbf{x}_i\right)}\right)^2}. \tag{30}$$

At present, there is no mathematical theory that proves the coefficient matrix, $\mathbf{W}$, is invertible. However, computational experience has shown that this matrix is invertible, provided the problem is well posed. Schaback and Hon [19] have demonstrated for elliptic PDEs that certain combinations of a constant shape parameter and knots can yield very ill-conditioned $\mathbf{W}$ matrices that from an implementation view be considered singular. However, the such severe ill-conditioning can be easily avoided by perturbing the constant shape parameter by a small amount. Kansa [7] observed that the use of a variable parameter distribution forced the rows of the matrix to be linearly independent; however, no theoretical guidelines have been provided at present for the variable shape parameter selection.

For illustration, consider an elliptic PDE defined on a unit square domain. At least one side must have either Dirichlet or Robin boundary conditions, i.e., the function or the function plus its derivative values must be specified on the boundary, or else by construction, the matrix $\mathbf{W}$ is singular.

Because $\mathbf{W}$ is a full matrix, the solution of the set of linear equations will suffer from ill-conditioning as the rank N of the matrix increases. Three methods will be presented in this paper, showing methods to circumvent this problem.

3. BLOCK PARTITIONING METHODS

Block partitioning methods are, in a sense, a precursor to domain decomposition methods that are commonly used in traditional numerical schemes. This discussion will focus upon two-dimensional Poisson equation problems, but the methods presented here generalize to higher dimensions.

A domain, Ω, is partitioned into smaller nonoverlapping subdomains, Ω_i, each having $N_i < N$ points per subdomain. The partitioning technique employed here is similar to the method described in [20]. The domain Ω in R^2 is subdivided into several nonintersecting sets of knots. These nonintersecting sets consist of smaller planes in R^2, curves in R^1 that contain the loci of the interface knots between adjacent planes, and the common intersection knots in R^0 of the intersecting curves. The set of subdomains are denoted by Ω_i^{aa}, the set of curves are denoted

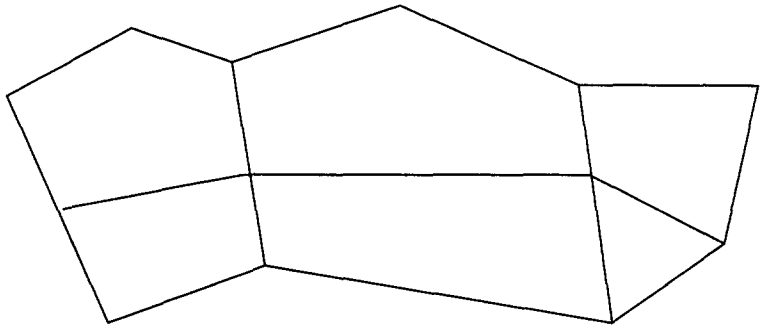

Figure 1. A schematic of a division of a domain into six nonoverlapping subdomains.

by Ω_i^{bb}, and the set of intersection points are denoted by Ω_i^{pp}. There will be i planes, j curves, and k intersection knots. The subdomains that couple knots in Ω_i^{aa} and knots in Ω_i^{bb} are denoted as Ω_i^{ab}. Similar relations exist for the other coupling sets.

The block partitioned algorithm presented will be for the general case in which the sets of curves, Ω_i^{bb}, and intersections, Ω_i^{pp}, are nonempty. Such sets are empty if they contain no knots as in the situation where the curves and intersection are between knots. Such a partitioning provides the flexibility of adding or deleting knots in entire domain; for efficient parallelization, the partitioning should be load-balanced as much as possible.

The global matrix $\mathbf{W}$ associated with this partitioning can be written as

$$\mathbf{W} = \begin{bmatrix} \mathbf{W}^{aa} & \mathbf{W}^{ab} & \mathbf{W}^{ap} & \mathbf{col}_a \\ \mathbf{W}^{ba} & \mathbf{W}^{bb} & \mathbf{W}^{bp} & \mathbf{col}_b \\ \mathbf{W}^{pa} & \mathbf{W}^{pb} & \mathbf{W}^{pp} & \mathbf{col}_p \\ \mathbf{row}_a & \mathbf{row}_b & \mathbf{row}_p & 0 \end{bmatrix}, \tag{31}$$

where $[\mathbf{row}_i] = [\mathbf{col}_i]^{\mathsf{T}}$ represents a zero or one depending if a knot is an interior point or a Dirichlet boundary point.

Each block submatrix, in turn, is composed of subblocks. $\mathbf{W}^{aa}$ will be composed of $i \times i$ subblocks, $\mathbf{W}^{ab}$ will be composed of $i \times j$ subblocks, $\mathbf{W}^{ap}$ will be composed of $i \times k$ subblocks, etc. For example, $\mathbf{W}^{aa}$ will have the following structure:

$$\mathbf{W}^{aa} = \begin{bmatrix} \mathbf{W}^{aa}(1,1) & \mathbf{W}^{aa}(1,2) & \cdots & \cdots & \mathbf{W}^{aa}(1,i) \\ \mathbf{W}^{aa}(2,1) & \mathbf{W}^{aa}(2,2) & \cdots & \cdots & \mathbf{W}^{aa}(2,i) \\ \cdots & \cdots & \cdots & \cdots & \cdots \\ \cdots & \cdots & \cdots & \cdots & \cdots \\ \mathbf{W}^{aa}(i,1) & \mathbf{W}^{aa}(i,2) & \cdots & \cdots & \mathbf{W}^{aa}(i,i) \end{bmatrix}. \tag{32}$$

Successive block LU decompositions and diagonalizations are performed. Although the operation count in constructing the inverse of the matrix is approximately the same if it were performed globally or by block elimination, the primary advantage of a block elimination scheme is that many sets of smaller blocks are much better conditioned, low rank matrices are used to construct the global inverse matrix. The other advantage is that parallelization can be permitted, because the diagonal subblocks are considerably smaller in rank, the condition numbers, K,

$$K = \left| \frac{\lambda_{\max}}{\lambda_{\min}} \right| \tag{33}$$

are considerably smaller than that of the global matrix, $\mathbf{W}$.

Begin the LU decomposition scheme with $\mathbf{W}^{aa}$, while simultaneously building its inverse matrix, $\mathbf{V}^{aa}$. Because there can be a loss of precision during block elimination upon the diagonal subblocks, iterative refinement is used to correct the inverse subblock. Note the elimination process is readily parallelized, especially with building the Schur complements.

After $\mathbf{W}^{aa}$ is converted into the identity matrix and $\mathbf{V}^{aa}$ is constructed, the off-diagonal matrices $\mathbf{W}^{ab}$ and $\mathbf{W}^{ap}$ are multiplied by $\mathbf{V}^{aa}$. Next, $\mathbf{W}^{ba}$ is eliminated, forming a new Schur complement matrix, $\mathbf{W}'^{bb}$. This matrix is diagonalized, and its inverse is constructed similarly, to $\mathbf{W}^{aa}$. $\mathbf{W}^{bp}$ is then multiplied by $\mathbf{V}^{bb}$.

Then the blocks $\mathbf{W}^{pa}$ and $\mathbf{W}^{pb}$ are eliminated, forming a new Schur complement, $\mathbf{W}'^{pp}$. $\mathbf{W}'^{pp}$ is diagonalized and its inverse is constructed. The entire matrix, $\mathbf{W}$, is now in upper triangular form. The process can proceed further to construct the global inverse matrix $\mathbf{V}$ if desired. A note of caution should be issued. Demmel *et al.* [21] show that the elimination of the off-diagonal blocks and formation of the Schur complements is only conditionally stable because pivoting is not employed. If the global matrix, $\mathbf{W}$, is very poorly conditioned, then the Schur complement block matrices may be very poorly conditioned. Regularization may be a way to circumvent this problem and will be investigated in the future.

Domain decomposition can also be performed iteratively. After diagonalizing the matrix, $\mathbf{W}^{aa}$, the solutions across the 1D curves and vertex points are often solved iteratively using the alternating Schwartz method, see [20]. A guess is made regarding the solution at the interfaces and points, and iterative procedure is constructed by which alternating Dirichlet and Neumann conditions in the normal direction are specified.

For this paper, the alternating Schwartz method was not employed because the matrices for the line and point are small in rank, having a negligible additional overhead. Such a study with the alternating Schwartz method with MQ-RBFs has already been published by Dubal [22].

4. SOME TEST RESULTS

In most applications of MQ, a constant shape parameter is assumed for simplicity. A constant shape parameter yields symmetric matrices that have nice mathematical properties. Madych [23] showed theoretically that for a constant c^2 MQ formulation, the interpolation is increasingly more accurate as c^2 increases. Madych further points out this is not possible with finite precision computers because of increasing matrix ill-conditioning due to the accumulation of round-off errors. Tarwater [24] showed that the RMS errors first decreased with increasing values of the shape parameter, c^2, until a minimum was reached. This value of c^2 was termed the optimal value of the shape parameter. Beyond the optimal value, the RMS errors increased rapidly with increasing values of c^2. This observed dependence of the RMS error upon the shape parameter is believed to be related to the condition number of the matrix.

In each of the examples throughout this paper, the matrix $\mathbf{W}$ was preconditioned by the diagonal. A thorough study of preconditioners for full matrices is beyond the scope of this paper.

The choice of an optimal constant MQ shape parameter had been studied by Carlson and Foley [25], Milroy *et al.* [26], Golberg and Chen [27], and Hickernell and Hon [28]. Although the recommendations of Madych [23] are valid, Carlson and Foley did show that the function being interpolated was an important consideration in determining the optimal constant shape parameter. Carlson and Foley recommended that a small constant shape parameter be used if the function varies rapidly, but a large shape parameter be used if the function has large radius of curvature such as the surface of a sphere.

An experiment was performed to determine the optimal constant shape parameter for the Poisson equation, $F_{xx} + F_{yy} = -32F$ having an exact solution, $F(x, y) = \cos(4x + 4y)$. A global search was performed to bracket the optimal constant shape parameter, c^2. Condition numbers were estimated by the routine DGECO; these estimated condition numbers are generally within a factor of three of the ratios of the absolute values of the largest to smallest eigenvalues of a matrix. The domain $[0, 1] \times [0, 1]$ was uniformly subdivided into 3, 5, 7, 8, 9, 11, 13, 15, 17 knots in each direction. Table 1 shows the dependence of the optimal shape parameter versus the total number of points, N^2.

Table 1. Optimal shape parameter versus N for a sample Poisson equation problem, $F_{xx} + F_{yy} = -32F$.

N	K (condition number)	c^2 (optimal constant)
9	1.6e2	0.1880
25	3.6e3	0.0680
49	3.8e4	0.0480
64	6.3e4	0.0340
81	1.2e5	0.0295
121	4.3e5	0.0233
169	1.3e6	0.0200
225	3.1e6	0.0160
289	6.9e6	0.0140

Note that the optimal value of the shape parameter decreases monotonically, but as expected the condition number increases as N increases.

In a separate study, the domain was covered by a uniform distribution of 11×11 knots. Table 2 presents the root mean square error, the maximum condition number, K, and the number of subdomains. The exact solution is an exponential function $F(x, y) = \exp(2x + 2y)$ that varies from 1.0 to about 55 over the domain. A constant optimal shape parameter was used in each case, but the domain was block partitioned into 1, 4, 9, and 25 planar subdomains.

Table 2. RMS errors and condition number for the Poisson equation, $F_{xx}+F_{yy} = 8F$, as a function of the number of planar subdomains.

Number of Subdomains	c^2	Maximum K	RMS Error
1	0.028	7.99e + 5	0.231
4	0.028	1.38e + 3	0.010
9	0.028	2.32e + 1	0.018
25	0.028	3.77e + 0	0.002

Similar behavior was observed for various test functions with varying numbers of knots. The finest substructuring had the smallest condition number and RMS errors. The RMS errors of the finest partitioning were two orders of magnitude smaller than the global matrix.

Kansa [6,7] found experimentally that a power-law shape parameter distribution worked well for functions that are strictly monotonic. He observed that the matrix condition number was favorably reduced because the rows of the matrix elements tended to have more distinct entries with a variable shape parameter distribution. Kansa argued that even though the variable shape parameter destroyed the matrix symmetry, it was worthwhile considering the substantial increases in accuracy and the lowering of the condition number.

Intuitively, it appears that a variable MQ shape parameter distribution ought to be related to the local curvature of the function being interpolated. The radius of curvature, $\rho(x_i, y_i)$, at a specific point, $\mathbf{x}_i$, was calculated by the principles of differential geometry. Because at very steep regions, $\rho(x_i, y_i)$ may become very large, hence, ρ was restricted to not exceed 1,000 to prevent severe ill-conditioning. By experimentation, it was found that c_j^2 in general had the following dependency:

$$c_j^2 = \begin{cases} k_1 + k_2 \rho(x_i, y_i), & \text{if } \rho(x_i, y_i) \leq 1{,}000, \\ k_1 + 1000 k_2, & \text{if } \rho(x_i, y_i) > 1{,}000. \end{cases} \tag{34}$$

The constants k_1 and k_2 will depend upon the total number of points over the domain. The value of k_1 can be estimated from the optimal value of a constant of c^2. Given the constant shape parameter solution, approximate partial derivatives are constructed to estimate the local

radius of curvature, and hence, the local shape parameter. The constant k_2 can be found by optimizing one parameter. A detailed study of these constants for a variety of test functions and number of knots is beyond the scope of this paper.

In the following exercise, a uniform 11×11 knot problem was studied with variable shape parameter. The global matrix was partitioned into 36 2D planes, 60 lines, and 25 vertex points. The constants k_1 and k_2 were optimized for the exponential solution having values of 0.025 and 0.070, respectively.

The same shape parameter relation, equation (34), was applied to the various test problems. Note, the condition numbers do vary depending on the test problem because the matrix elements have a dependence upon the local shape parameter. The condition number of the global matrix without substructuring ranged from $3.0e+10$ to $4.0e+12$. These calculations using a variable shape parameter were performed on a computer whose machine limit of condition number is approximately $4e+12$. The matrices generated from a constant shape parameter with very large constant shape parameters had such large condition numbers that linear equation solver was unstable.

Note, from Table 3, as the test functions vary more rapidly, the functions $F(4x+4y)$ are in general less accurate than the slower varying functions $F(2x+2y)$. The explanation for this is that the uniform knot distribution of 121 points is not optimal. If the knot locations do not follow the extrema and inflection points, an undersampling will result. In contrast, Hon and Mao [13] showed that with only ten knots and an adaptive knot strategy, MQ can produce very accurate results for the Burgers' equation with Reynolds number of 10,000.

Table 3. The maximum condition number and RMS errors for 12 test functions using a variable shape parameter distribution, equation (34), and matrix substructuring.

Function	Max K	RMS Error
$\exp(2(x+y))$	12.5	$7.46e-4$
$\exp(4(x+y))$	48.4	$1.53e-2$
$\cos(2(x+y))$	13.5	$1.32e-4$
$\cos(4(x+y))$	31.9	$2.46e-4$
$\sin(2(x+y))$	3.33	$5.19e-4$
$\sin(4(x+y))$	27.3	$5.62e-4$
$\log(2(x+y)+1.e-7)$	4.47	$2.48e-2$
$\log(4(x+y)+1.e-7)$	16.9	$4.26e-2$
$\exp\left(2\left(\left(x-\frac{1}{2}\right)^2+\left(y-\frac{1}{2}\right)^2\right)\right)$	207.86	$4.74e-4$
$\exp\left(4\left(\left(x-\frac{1}{2}\right)^2+\left(y-\frac{1}{2}\right)^2\right)\right)$	4.8	$9.16e-3$
$\arctan(2(x+y))$	118.1	$1.85e-4$
$\arctan(4(x+y))$	30.5	$9.09e-4$

As the number of knots increases, the values of k_1 and k_2 were adjusted to keep the global matrix (without substructuring) stable. For a problem of 15×15 knots (225 knots), the optimal value of k_1 and k_2 were $4.45e-3$ and 0.162, respectively. The test problem was $F_{xx}+F_{yy}=-32F$, $(F(x,y)=\cos(4x+4y))$. With this choice of parameters, the global condition number was $1.4e+11$, and the global RMS error was 0.064. However, the same problem solved by block partitioning and substructuring yielded a maximum block condition number of 867, but an RMS error of 0.00013.

Not all the tests were reported here, but in general, the results show that when either a constant or variable shape parameter distribution values are pushed near the limits of machine

precision, the block partitioned method described here has matrix condition numbers many orders of magnitude smaller than that of the global matrix. Most importantly, because the round-off error contamination of the expansion coefficients are negligibly small with block-partitioning, the RMS errors are consistently about two to three orders of magnitude smaller. Thus, by reducing the accumulated effect of round-off errors by suitably fine block partitioning, substantial gains in accuracy can be achieved.

5. CONSTRUCTION OF TRUNCATED T-MQ-RBFS

Even though Franke [2] demonstrated that global RBF methods were superior to the commonly used, compactly supported interpolation schemes, the debate still continues whether it is better to use compactly supported approximations or globally supported RBFs for large scale computations. The main impetus behind this debate is the problem with full ill-conditioned matrices. Matrix sparcity, however, is not the entire remedy because FEM using compactly supported basis functions still can give rise to poorly conditioned matrices.

Because MQ-RBFs are continuously differentiable everywhere for all $c_j^2 > 0$, it would be desirable to construct a truncated RBF that is also continuously differentiable. The MQ basis function tends asymptotically toward a linear function for large values of $r = \|\mathbf{x} - \mathbf{x}_j\|$. Because the MQ-RBF is a consistent solution to the biharmonic potential problem, see [4], such a solution has a finite range over which its influence is significant. The exercise presented here is an attempt to find the range of significant influence to yield matrices with finite, rather than full band-widths.

A truncated T-MQ basis function was constructed such that

$$g\left(\|\mathbf{x}-\mathbf{x}_j\|\right) = \begin{cases} \sqrt{\|\mathbf{x}-\mathbf{x}_j\| + c_j^2}, & \text{if} \quad r \le r_{\text{cutoff}}, \\ \eta(r)\sqrt{\|\mathbf{x}-\mathbf{x}_j\| + c_j^2}, & \text{if} \quad r > r_{\text{cutoff}}, \end{cases} \tag{35}$$

where

$$\eta(r) = \frac{(r + r_{\text{cutoff}})}{(2r_{\text{cutoff}})} \exp\left(-k_3 \left|r - r_{\text{cutoff}}\right|\right). \tag{36}$$

The decay function, $\eta(r)$, is set to zero if its magnitude is less than 0.001, yielding zero matrix coefficient elements. In the following study, a constant shape parameter distribution was used for the full matrix having the value of $c_j^2 = 0.072$ over a unit square with 121 evenly distributed knots. The test problem was $F_{xx} + F_{yy} = -32F$, $(F(x,y) = \cos(4x + 4y))$. Over the unit square, 121 evenly spaced knots were used with a total of 25 subdomains. The decay constant, k_3, was set to 10.0. Table 4 shows the relation among parameter, r_{cutoff}, the global and the subpartitioned RMS errors.

Table 4 shows the sensitivity of the cutoff distance and the RMS errors. The maximum point separation on a unit square is $\sqrt{2} = 1.414$, representative of a full matrix. The RMS errors appear to have saturated at the full matrix shape parameter value of 0.072, having RMS errors of $3.8e-4$ at a cutoff distance of 1.3. Those cutoff distances smaller than 1.3 begin to diverge. However, below the cutoff distance of 1.3, the RMS errors can be reduced further by optimizing the shape parameter. There is a tradeoff between matrix band-width and accuracy that needs to be considered.

Under the same decay function, $\eta(r)$, and the test problem, the computation was performed using a variable c_j^2 distribution, see equation (34). In Table 5, the parameters were optimized to obtain the lowest possible RMS errors.

It is clear, from Table 5, that the form of the T-MQ obtained from equation (35) with a variable c_j^2 distribution is superior in the reduction of error than using a constant shape parameter distribution. The conclusion still remains that as the T-MQ approaches a more global approximation and the coefficient band-width increases, the RMS errors decrease, but the condition number

Table 4. The relation among parameter, r_{cutoff}, the constant shape parameter, and the subpartitioned RMS errors.

r_{cutoff}	RMS Error ($c^2 = 0.072$)	Adjusted c^2	RMS Error (Adjusted c^2)
1.414	3.8e − 4	0.072	3.8e − 4
1.40	3.8e − 4	0.072	3.8e − 4
1.30	3.8e − 4	0.072	3.8e − 4
1.25	2.3e − 3	0.061	1.3e − 3
1.20	6.5e − 2	0.0709	6.6e − 3
1.10	3.0e + 0	0.0738	6.65e − 1

increases along with the computational complexity. Whether equation (35) is the optimal form for a T-MQ RBF and the shape parameter distribution is an open question.

To further illustrate the relation between the r_{cutoff} and the RMS error, under the same test problem, a numerical computation was performed by using the variable shape parameter with $k_1 = 1.\text{e} - 6$ and $k_2 = 0.05$ and 289 evenly spaced knots over a total of 25 subdomains. Table 6 gives the relation between the r_{cutoff} and the subpartitioned RMS errors.

Table 5. The relation among parameter, r_{cutoff}, the variable shape parameter distribution, and the subpartitioned RMS errors.

r_{cutoff}	k_1	k_2	RMS Error
1.414	4.45e − 3	0.162	0.0002
1.275	4.45e − 3	0.162	0.0002
1.15	0.09	0.136	0.0021
1.10	0.077	0.133	0.0059
1.05	0.037	0.116	0.0069

Table 6. The relation between r_{cutoff} and the subpartitioned RMS errors.

r_{cutoff}	Max Condition Number	RMS Error
1.414	39.37	8.92e − 5
1.25	23.14	4.07e − 4
1.20	21.59	4.08e − 4
1.05	18.26	1.24e − 3
1.00	18.03	2.10e − 3

In contrast to the 11 × 11 case (see Table 4), this 17 × 17 case yields acceptable RMS errors, 2.10e − 3, even with a $r_{\text{cutoff}} = 1.00$ compared with the 11 × 11 case with RMS errors of 6.65e − 1. The result indicates that the performance of the truncated T-MQ basis function can be improved for increasingly smaller truncation distances (matrix band-widths) by optimizing the constants k_1 and k_2 of the variable shape parameter distribution as well as by increasing the number of knots. When the number of knots is increased, such as the 17 × 17 case, an $r_{\text{cutoff}} = 1$ performs very well. Clearly, more investigation is required for large scale problems. But based on this limited study, it is possible to speculate that MQ can be applied to large scale problems if a truncated T-MQ expansion is used, and the shape parameter distribution parameters are optimized. Furthermore, many of the linear algebra tools developed by the FEM community could be used in a truncated MQ context.

It can be concluded that a variable c_j^2 distribution with a finer resolution is required for obtaining a coefficient matrix with small band-width. The advantage of a truncated T-MQ

method yielding narrower coefficient matrices is that the growth of the condition number with rank can be controlled and fewer operations are required when the matrix has progressively more zero elements. The optimal balance between the number of knots and matrix band-width for a desired degree of accuracy is a subject for future investigation.

Chen *et al.* [29] used the compactly support RBFs of Wendland [30] to solve various PDEs such as the Poisson equation in two dimensions. They found that by adjusting the band-width of the coefficient matrix, the accuracy of the solution could be tuned for a given number of knots. As the band-width increased towards that of a full matrix, the better became the accuracy. A compromise of quality of solution and computational efficiency needs to be chosen for a particular application. Likewise, the order of polynomials and degree of continuity is also an important consideration in improving accuracy and efficiency. While higher-order polynomials have higher convergence rates, they can suffer from potential instabilities.

The results in Table 4 are consistent with the results of Chen *et al.* [29] who included compactly supported RBFs into boundary element methods. For the choice of the decay factor of the truncated T-MQ, it is seen that the full matrix is not necessary to achieve high accuracy. This choice of a truncated T-MQ may be preferable to higher-order polynomial schemes that can suffer from the notorious polynomial snaking problem. Clearly, more numerical and theoretical studies are required to obtain the best balance between accuracy and computational efficiency.

6. MULTIZONE METHODS

Wong *et al.* [31] implemented a multizone method for implementing the PDE simulation of the two-dimensional time dependent shallow water equations in Tolu Harbor, Hong Kong. The entire domain was partitioned into a finite number of nonoverlapping zones. Over each zone the MQ method is applied similar to the global MQ simulation. However, the resulting matrix for each zone has considerably fewer points, hence, are better conditioned.

Although this scheme was implemented on a serial computer, there was a gain to 42 and 50% in efficiency in the five and seven zone scheme, respectively. To maintain continuity across the zone boundaries, two additional sets of knots were appended to the zone. The first set of knots includes all points that are in other zones and adjacent to the boundary of Ω^i. The other set of knots are chosen at random such that they are sparsely and evenly distributed over the other zones of Ω. The entire set of knots forms the inflated zone Ω^i. The expansion coefficients over the inflated zone are solved. However, the functions and their partial derivatives pertinent to the zone Ω^i, excluding those from the inflated zone are calculated. From the values of the functions and their partial derivatives, the time marching solution is generated.

This multizone approach has been able to calculate time dependent solutions of the shallow water equations applied to the Tolu Harbor during the period between February 1, 1991 and April 30, 1991 with accuracies comparable or even more accurate than the global matrix approach. Table 7 shows the accuracies and efficiencies of the multizone method over the global MQ simulation for a total of 210 and 260 points, respectively, see [31]. The multizone approach also permits implementation on parallel computers.

Table 7. The RMS errors and CPU times on computing the tidal level of the Tolu Harbor by using the global and multizone MQ methods.

	RMS Error (m)	CPU Time (Secs)
260 global nodes	7.615e − 2	993
210 global nodes	1.058e − 1	706
5 subzones	7.906e − 2	575
7 subzones	7.570e − 2	481

7. DISCUSSION

This paper has presented several ideas to solve PDEs with MQ-RBFs that circumvent the ill-conditioning problems associated with a global mesh-free approximation scheme. These ideas are: domain decomposition/block subpartitioning, variable MQ shape parameters related to the local radius of curvature, a truncated MQ basis function with a finite band-width, a multizone method, preconditioning, and adaptive, optimal knot distributions. Combinations of one or more of these considerations that improve the conditioning of the coefficient matrices also improve the accuracy of the solutions.

Although there is an infinite class of possible global and compactly-supported RBFs, the MQ-RBF is known to possess exponential convergence. Its primary disadvantage is that it is a global approximation scheme that gives rise to full matrices. Hardy [4] had recognized this disadvantage, and showed domain decomposition with blending is a method to circumvent this disadvantage and still obtain highly accurate results. Franke [2] compared global RBF interpolation schemes with many popular compactly supported schemes, and found that the global RBF schemes were superior on six criteria.

Madych [23] showed theoretically that the MQ interpolation scheme converges faster as the constant MQ shape parameter becomes progressively larger. But because finite precision computers are used, the system of equations becomes progressively more ill-conditioned as the shape parameter increases until numerical instability occurs.

The following outlines the methods proposed in this paper.

- Block substructuring and partitioning yields block matrices of considerably smaller rank are several orders of magnitude better conditioned than the global matrix. The resulting numerical solutions can be more accurate by a few orders of magnitude. Parallelization can be readily introduced.
- Simple preconditioners improve the condition number of large matrices. A preconditioner should be a simple, easily calculated approximation to the inverse of the matrix. This is still an unresolved issue that requires more research.
- A variable MQ shape-parameter recipe based upon the local radius of curvature yields better conditioned matrices and more accurate solutions than a constant shape parameter MQ scheme. The condition numbers of both the global and partitioned blocks are smaller because the rows of the matrix elements are more distinct, but the RMS errors can be one to two orders of magnitude less than the accepted constant shape parameter MQ scheme.
- Transform the global MQ basis function into a truncated basis function. By multiplication by an exponentially decaying function, the resulting matrix has a finite, rather than a full band-width. The T-MQ-RBF that was constructed from transcendental functions is continuously differentiable. A balance between efficiency and accuracy will require optimization.
- The multizone method of Wong *et al.* [31] is yet another alternative method improving computational efficiency and parallelization. Smaller rank subdomains are independently solved that include knots from other subdomains. Not only is this method readily parallelized, but the conditioning of the resulting matrices is much better and the results are comparable to the global approximation scheme.
- Optimization of knot location requires many fewer knots and better conditioned matrices, and yields superior accuracy. Hon and Mao [13] showed that an adaptive algorithm that adjusted the knots to follow the peak of the shock wave can produce extremely accurate results in 1D with only 10 knots, even for extremely steep shocks with $\mathrm{Re} = 10,000$.
- Multilevel approximation schemes developed by Fasshauer and Jerome [32] can be used with T-MQ-RBF to keep the band-width constant, but refine spatial regions to the desired degree of accuracy.

It is recommended that a hybrid combination of these above-method techniques be considered in solving PDEs. It is the goal of any method to produce the results having the best accuracy with least expenditure of effort for increasingly more complex problems.

8. CONCLUSION

There are no magic answers to the problem of simulating large scale complex PDE problems. The FEM method has been widely used because it used simple polynomial approximations with compact support. Even though FEM has compact support, the resulting coefficient matrices even with finite band-widths can still be ill-conditioned. The lessons learned by the many researchers in FEM can be applied to RBFs.

We show that there are alternate approaches to the problems of larger simulation that we adapted from standard FDM, FEM, and FVM. Namely, a large global matrix is best treated by various themes and variations of the established domain decomposition methods. Just by reducing the round-off contamination, RMS errors can be reduced several orders of magnitude.

Einstein once said, "Imagination is more important than knowledge." His advice should be heeded when it comes to the problem of solving large scale PDE problems. It is too premature to dismiss global RBF scheme as MQ because there are alternate methods that within a hybrid scheme could circumvent the problem of global matrices and ill-conditioning. With some imagination and further research, the issues raised in this paper could provide an efficient alternate to FEM. In addition, there is an infinite class of possible RBFs either with either global, compact, or hybrid combination that still needs to be explored.

REFERENCES

1. W.R. Madych and S.A. Nelson, Multivariable interpolation and conditionally positive definite functions II, *Math. Comp.* **54**, 211–230, (1990).
2. R. Franke, Scattered data interpolation: Tests of some methods, *Math. Comput.* **38**, 181–199, (1972).
3. R.L. Hardy, Multiquadric equations of topography and other irregular surfaces, *J. Geophys. Res.* **76**, 1905–1915, (1971).
4. R.L. Hardy, Theory and applications of the multiquadric-biharmonic method: 20 years of discovery, *Computers Math. Applic.* **19** (8/9), 163–208, (1990).
5. J. Duchon, Spline minimizing rotation-invariant seminorms in Sobolev space, In *Constructive Theory of Functions of Several Variables, Lecture Notes in Mathematics, Volume 571*, Springer-Verlag, Berlin, (1977).
6. E.J. Kansa, Multiquadrics—A scattered data approximation scheme with applications to computational fluid dynamics—I. Surface approximations and partial derivative estimates, *Computers Math. Applic.* **19** (8/9), 127–145, (1990).
7. E.J. Kansa, Multiquadrics—A scattered data approximation scheme with applications to computational fluid dynamics—II. Solutions to hyperbolic, parabolic, and elliptic partial differential equations, *Computers Math. Applic.* **19** (8/9), 147–161, (1990).
8. M.A. Golberg and C.S. Chen, The theory of radial basis functions used in the dual reciprocity boundary element method, *Appl. Math. Comp.* **60**, 125–136, (1994).
9. M. Sharan, E.J. Kansa and S. Gupta, Applications of the multiquadric method for the solution of elliptic partial differential equations, *Appl. Math. Comput.* **84**, 275–302, (1997).
10. M.A. Golberg and C.S. Chen, Discrete projection methods for integral equations, Comput. Mech., Boston, MA, (1997).
11. Y.C. Hon and X.Z. Mao, A multiquadric interpolation method for solving initial value problems, *Sci. Comput.* **12** (1), 51–55, (1997).
12. Y.C. Hon, M.W. Lu, W.M. Xue and Y.M. Zhu, Multiquadric method for the numerical solution of a biphasic model, *Appl. Math. Comput.* **88**, 153–175, (1997).
13. Y.C. Hon and X.Z. Mao, An efficient numerical scheme for Burgers equation, *Appl. Math. Comput.* **95**, 37–50, (1998).
14. Y.C. Hon, K.F. Cheung, X.Z. Mao and E.J. Kansa, A multiquadric solution for shallow water equation, *ASCE J. Hydraulic Engineering* **125** (5), 524–533, (1999).
15. Y.C. Hon and X.Z. Mao, A radial basis function method for solving options pricing model, *Financial Engineering* **8** (1), 31–50, (1999).
16. Z.M. Wu, Hermite-Bikhoff interpolation of scattered data by radial basis function, *Approximation Theory and its Application* **8**, 1–10, (1992).

17. Z.M. Wu, Solving PDE with radial basis function and the error estimation, In *Advances in Computational Mathematics, Lecture Notes on Pure and Applied Mathematics, Volume 202*, (Edited by Z. Chen, Y. Li, C.A. Micchelli, Y. Xu and M. Dekker), GuangZhou, (1998).
18. M.R. Dubal, S.R. Olivera and R.A. Matzner, In *Approaches to Numerical Relativity*, (Edited by R.D. Inverno), Cambridge University Press, Cambridge, UK, (1993).
19. R. Schaback and Y.C. Hon, On unsymmetric collocation by radial basis functions, *Appl. Math. Comput.*, Preprint (1999) (to appear).
20. B. Smith, P. Bjorstad and W. Gropp, *Domain Decomposition: Parallel Multilevel Methods for Elliptic Partial Differential Equations*, Cambridge University Press, Cambridge, UK, (1996).
21. J.W. Demmel, N.J. Higham and R.S. Schreiber, Stability of block LU factorization, *Numer. Lin. Algebra Applic.* **2** (2), 173–190, (1995).
22. M.R. Dubal, Domain decomposition and local refinement for multiquadric approximations. I. Second-order equations in one-dimension, *Int. J. Appl. Sci. Comput.* **1** (1), 146–171, (1994).
23. W.R. Madych, Miscellaneous error bounds for multiquadric and related interpolants, *Computers Math. Applic.* **24** (12), 121–138, (1992).
24. A.E. Tarwater, A parametric study of Hardy's multiquadric equations for scattered data interpolation, UCRL-54670, (1985).
25. R.E. Carlson and T.A. Foley, The parameter R2 in multiquadric interpolation, *Computers Math. Applic.* **21** (9), 29–42, (1991).
26. M.F. Milroy, G.W. Vichers and C. Bradley, An adaptive radial basis function approach to modeling scattered data, *J. Appl. Sci. and Comput.* **1** (2), 319–349, (1994).
27. M.A. Golberg and C.S. Chen, Improved multiquadric approximation for partial differential equations, *Engr. Anal. with Bound. Elem.* **18**, 9–17, (1996).
28. F.J. Hickernell and Y.C. Hon, Radial basis function approximation of the surface wind field from scattered data, *Appl. Sci. Comput.* **4**, 221–247, (1998).
29. C.S. Chen, C.A. Brebbia and H. Power, Boundary element methods using compactly supported radial basis functions, *Comm. Numer. Meth. Engng* **15**, 137–150, (1999).
30. H. Wendland, Piecewise polynomial, positive definite and compactly supported radial basis functions of minimal degree, *Adv. Comput. Math.* **4**, 389–396, (1995).
31. S.M. Wong Y.C. Hon, T.S. Li, S.L. Chung and E.J. Kansa, Multizone decomposition for simulation of time-dependent problems using the multiquadric scheme, *Computers Math. Applic.* **37** (8), 23–43, (1999).
32. G. Fasshauer and J. Jerome, Multistep approximations algorithms: Improved convergence rates through postconditioning with smoothing kernals, *Adv. Comp. Math.* **10**, 1–27, (1999).
33. C.A. Micchelli, Interpolation of scattered data: Distance matrices and conditionally positive definite functions, *Constr. Approx.* **2**, 11–22, (1986).